www.czasopisma.pan.pl PAN POLSKA AKADEMIA NAUK www.journals.pan.pl

Arch. Metall. Mater. **68** (2023), 1, 89-96

DOI: https://doi.org/10.24425/amm.2023.141478

BARIŞ KARABAYRAK[1*], SINEM BASKUT[2], DILEK TURAN[1]

INVESTIGATION OF THE MECHANICAL PROPERTIES OF CALCIUM TREATED LOW CARBON STEEL

In this study, the effect of calcium treatment on the mechanical properties and fatigue behavior of low carbon steel material is investigated. By applying calcium treatment after aluminum deoxidation for steel cleanliness, the aim is to transform the inclusions into harmless structures and produce cleaner liquid steel. As a result of the study, calcium treated material's tensile strength slightly increases while fatigue life decreases. SEM studies were conducted to evaluate the results and it was observed that while elongated inclusions were observed as well as spherical shapes in the untreated sample, the inclusions generally had a spherical shape in the calcium treated sample. After the steel cleanliness process, the mechanical properties of the samples were improved. The tensile strength of the calcium treated sample increased slightly. However, a significant decrease in fatigue strength was observed depending on brittle inclusions that occur as a result of the calcium treatment process.

Keywords: Clean steel; Inclusion; Tensile strength; Fatigue; Microstructure

1. Introduction

Steel cleanliness is an important factor of steel quality and the demand for clean steel is increasing. Clean steel contains low amounts of non-metallic inclusions, such as oxygen, sulfur, phosphorus, hydrogen, nitrogen and even carbon, and the level of cleanliness is determined by the amount of inclusion of these substances in the steel [1]. To obtain clean steel, inclusions are reduced or modified to harmless inclusions during a ladle metallurgy process between steel production and casting. In the continuous casting stage, it is desirable to maintain the level of steel cleanliness achieved.

Inclusions inside the steel are of two types: internal and external. Internally generated inclusions are composed of reactions during steel production while external inclusions are inclusions resulting from external factors, such as slag and refractories. Non-metallic inclusions negatively affect steel properties, such as tensile strength, workability, toughness, weldability, fatigue resistance, and corrosion resistance.

The effect of inclusions on steel quality varies according to the shape, number, size, and distribution of inclusions [2,3]. Generally, controlling oxide and sulfide levels is important for steel cleanliness. Total oxygen content, the sum of the oxygen content in steel for dissolved oxygen and oxygen in inclusions, is extremely important in terms of steel cleanliness. The oxygen content of steel should be as low as possible because low oxygen content reduces the possibility of unwanted large oxide inclusions [1].

During the production process of steel, deoxidation (oxygen removal) is carried out in a ladle metallurgy process and the amount of oxygen is drawn to certain levels. In steelmaking processes, there are primarily three elements (silicon, manganese, and aluminum) used in steel deoxidation. Calcium, which is a highly reactive element, is used for modify the morphology of inclusions and calcium treatment is a way to modify solid alumina inclusions to liquid calcium-aluminates [4,5].

In steel production, nozzle clogging problems are encountered in the continuous casting process and solid Al_2O_3 inclusions have been found in the nozzle [6]. With the development of calcium injection techniques, the effects of calcium in the steel melt have been clarified [7]. The first comprehensive study on steel cleanliness control was conducted by Kiessling [1]. Later on, Mu and Holappa [8], Cramb [9], Zhang and Thomas [10] conducted studies on steel cleanliness.

Al_2O_3 and MnS inclusions occur during continuous casting and during solidification in deoxidized steels with Al; they were found to have a negative effect on the mechanical and physical properties of the final product [11,12]. For steels untreated with calcium, during rolling, MnS inclusions show elongation

[1] ESKISEHIR TECHNICAL UNIVERSITY, FACULTY OF AERONAUTICS AND ASTRONAUTICS, DEPARTMENT OF AIRFRAME AND POWER PLANT MAINTENANCE, ESKISEHIR, TURKEY
[2] ESKISEHIR TECHNICAL UNIVERSITY, FACULTY OF ENGINEERING, DEPARTMENT OF MATERIALS SCIENCE AND ENGINEERING, ESKISEHIR,TURKEY

* Corresponding author: bariskarabayrak@eskisehir.edu.tr

in the rolling direction while Al_2O_3 inclusions are broken in the rolling direction. By applying calcium treatment to the steel, non-deformable spherical inclusions are obtained during rolling [13,14]. Calcium can modify oxide and sulfide inclusions. However, insufficient calcium addition leads to incomplete modification of alumina inclusions and consequent formation of solid calcium aluminates having high melting points. These are detrimental to the castability of steel. On the other hand, excess calcium addition leads to the formation of a large number of CaS inclusions and partially modified calcium aluminate inclusions deteriorating castability of steel besides adverse effects on physical and mechanical properties on final product [14]. Moreover, oxide-sulfide duplex inclusions are always observed in the steel [15]. Duplex inclusions containing calcium and aluminum such as $CaO(Al_2O_3)$ and $CaO(Al_2O_3(2SiO_2))$ are thought to be most detrimental to the fatigue strength [16].

Studies have been carried out on steel cleanliness with calcium treatment and new methods are being developed [17,18]. The fatigue behavior of steel varies depending on many factors, such as size, shape and number of inclusions, and the bond with the matrix material. These factors are related to the stress concentration factor and the stress distribution around the inclusion. Inclusion size has a major effect on fatigue strength. Inclusions with an irregular shape and sharp edges cause larger stress concentrations around the inclusions than inclusions with a smooth shape, making it easier for a fatigue crack to initiate. Differences in the thermal expansion coefficients of the inclusion and the matrix can generate internal stresses around inclusions.

Studies on the effect of steel cleanliness on the fatigue properties of steel have been carried out [16, 19-25]. The aim of this study is to investigate the effects of steel cleanliness with calcium treatment on the mechanical properties of low carbon steel material. In this context, fatigue tests of the materials under constant amplitude axial loads have been performed.

2. Experimental procedures

2.1. Material and methods

The chemical composition of the low carbon steel material, obtained from industry, used in experimental studies is given in TABLE 1.

TABLE 1

Chemical composition of low carbon steel material (weight %)

C	Mn	P_{max}	S_{max}	Al
0.14-0.18	0.85-1.05	0.035	0.035	0.02-0.06
Ca (ppm)	**Ti_{max}**	**Cr_{max}**	**Mo_{max}**	**Fe**
20-60	0.010	0.080	0.020	Balance

Calcium treated and untreated materials were obtained from industry. Both of the untreated steel samples and calcium treated steel samples were produced in the same batch. Ladle furnace outlet temperature was 1579°C in average and casting speed was 1.1 m/min in the casting process. The slab thickness, width and length were measured as 200 mm, 1230 mm and 5860 mm, respectively. The final product analysis is S275JRC quality according to EN 10025-2:2004 standard. The materials are hot rolled. The materials were rolled into 13.8 thicknesses. Tensile and fatigue tests of both materials were performed to determine the effect of the calcium treatment for steel cleanliness on the mechanical properties of the material. Tensile tests were carried out by using four samples for both untreated steel and calcium treated steel. Fatigue tests were carried out by using thirteen samples for both untreated steel and calcium treated steel.

Tensile test samples were prepared according to ASTM E8 standards, and fatigue test specimens were prepared according to ASTM E466 standards. The dimensions of the tensile and fatigue test samples are given in Fig. 1.

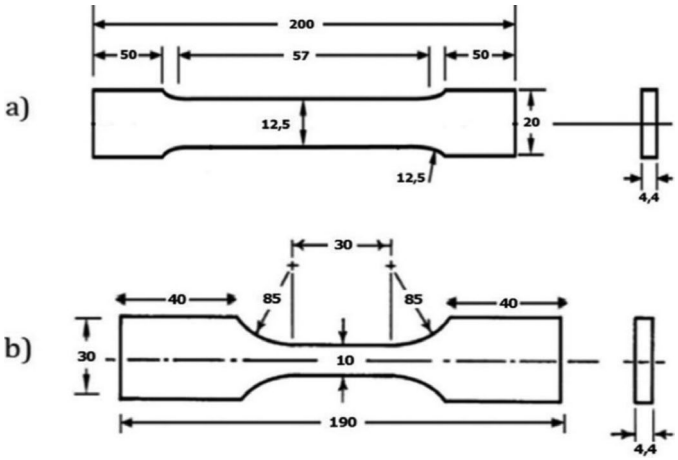

Fig. 1. Standard sample sizes: (a) Tensile test. (b) Fatigue test (dimensions given in mm)

The cyclic fatigue tests were performed on a servo-hydraulic mechanical test machine (INSTRON Model 8501) equipped with a 100 kN load cell. The stress amplitude-controlled high cycle fatigue tests were performed using a sinusoidal waveform at a stress ratio (R = minimum stress/maximum stress) of $R = 0.1$, and the maximum stresses were 400, 375 and 350 MPa. The frequency was chosen as 15 Hz in order not to affect the results of the fatigue tests with this value being applied for all of the fatigue tests. In all the fatigue tests, the applied load is in the form of a sinusoidal curve with the fatigue tests being performed until the sample broke.

2.2. Sample preparation and microscopic characterization

For microscopic investigations, the fractured parts after the fatigue tests were cut using a diamond disc in a precision cutting device (STRUERS Secotom-10). Cut surfaces were molded with Bakelite (STRUERS LaboPress-3) and mechanically polished from coarse to fine with diamond polishing solutions

and suitable polishing clothes by using an automatic polisher (STRUERS TegraPol-25). Following the polishing step, some of the selected samples were etched with a 5% nitric acid and 95% ethanol (Nital 5%) solution for about ten seconds in order to reveal the grain boundaries. Some of the polished samples were examined by using the light microscope (Zeiss PrimoTech). Additionally, to determine the changes in the internal structure, polished, polished+chemically etched and fractured surfaces of the untreated and calcium treated samples were examined in the scanning electron microscope (SEM, Zeiss SUPRA 50 VP) by using secondary electron (SE-SEM) imaging technique. Chemical analyzes of the inclusions on the polished surfaces were performed with the energy dispersive x-ray spectroscopy (EDS, Oxford Instruments, INCA ENERGY) attached to the SEM. The sizes of the inclusions were calculated with ImageJ software using more than ten backscatter electron (BSE-SEM) images taken from different regions in the microstructures of each sample's polished surfaces. In addition, the volume percentages of the inclusions were measured using more than ten BSE-SEM images taken at 5000× magnification from polished surfaces. Inclusion volume fractions were calculated using the equation (1) given below [26,27]:

$$X_0 = 0.89 R_0 f^{-1/3} \tag{1}$$

where X_0 is the average adjacent inclusion distance, R_0 is the true average inclusion radius and f is the inclusion volume fraction. X_0 is calculated from equation (2) [28]:

$$X_0 = 0.554 (N_v)^{-1/3} \tag{2}$$

where N_v is the number of inclusions per unit volume and derived from equation (3) [29]:

$$N_a = 2 R_0 N_v \tag{3}$$

where N_a is the number of inclusions per unit area on polished surfaces.

R_0 is determined by the following equation [26,30]:

$$(\pi/4) H(d) \tag{4}$$

where $H(d)$ is the harmonic average value of inclusion diameters measured from polished surfaces.

3. Results and discussion

3.1. Mechanical test results

Tensile tests were carried out by using four samples for both untreated steel and calcium treated steel. The average of the tensile test results of the untreated and the calcium treated samples are shown in Fig. 2. The tensile test results of untreated and calcium treated samples are given in TABLE 2. Tensile strength of calcium treated steel sample is marginally higher than untreated steel sample while strain deformation value is lower.

As can be seen in the results given in TABLE 2, the calcium treated sample's tensile strength increased slightly while elongation decreased.

TABLE 2

Effect of calcium treatment on tensile test results

Measured values	Untreated sample	Calcium treated sample
Tensile strength (MPa)	456 (±5)	492 (±2)
Maximum strain (%)	31.6 (±3)	27.8 (±3)

Fatigue tests were carried out by using thirteen samples for both untreated steel and calcium treated steel. Average of the fatigue test results of untreated and calcium treated samples for each maximum stress value are given in TABLE 3. As can be seen in the results given in TABLE 3, fatigue life significantly decreased with an increase of maximum stress in cyclic loads applied at $R = 0.1$. In tests where maximum stress of 350 MPa was applied, life in the untreated sample was 9.684.577 cycles, whereas in the case of maximum stress of 400 MPa, it decreased

TABLE 3

Effect of calcium treatment on fatigue test results

Maximum stress (MPa)	Number of cycles up to break (Untreated sample)	Number of cycles up to break (Calcium treated sample)
400	266.097 (±36.400)	196.424 (±18.600)
375	647.748 (±66.700)	274.901 (±25.800)
350	9.684.577 (±315.400)	1.048.561 (±167.900)

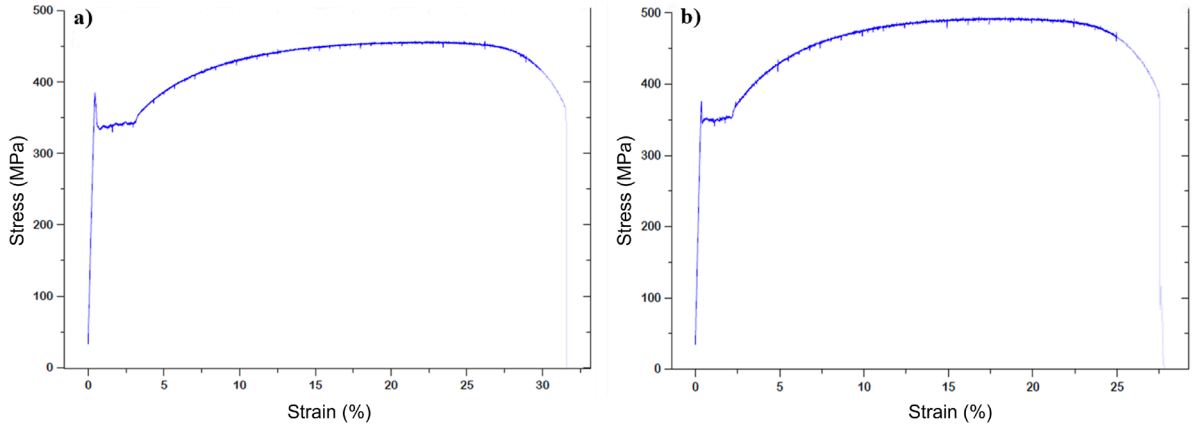

Fig. 2. Tensile test results: (a) Untreated steel sample. (b) Calcium treated steel sample

to 266.097 cycles. Similar results are observed in other tests. In addition, the results of the fatigue test on the calcium treated samples were lower than the fatigue test results of the untreated samples.

The variation of fatigue life with stress amplitude (S-N curves) for the untreated and the calcium treated samples created according to the fatigue test results are shown in Fig. 3. As can be seen from the S-N diagram, the degradation in cyclic fatigue life at the higher stress amplitudes and resultant short fatigue life than at the lower stress amplitudes and resultant enhanced fatigue life. In Fig. 3, it is seen that the fatigue life is lower for all stress values in calcium treated samples.

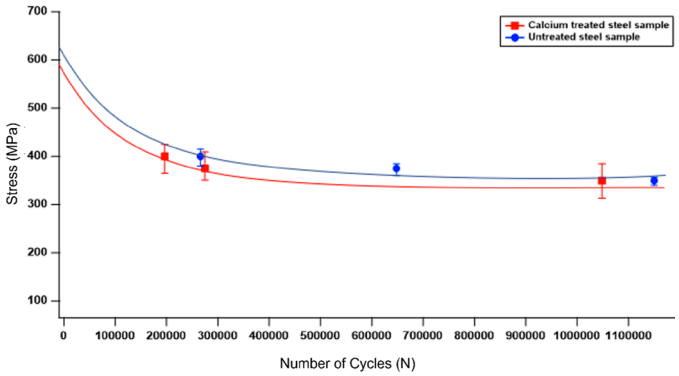

Fig. 3. S-N curves for the untreated and the calcium treated samples

3.2. Microstructure investigations

The purpose of the calcium treatment after aluminum deoxidation is to modify inclusions and produce cleaner liquid steel. It was expected that the calcium treatment process would improve the mechanical properties of the material. The tensile strength value of the calcium treated materials was slightly increased. However, in this study, the fatigue strength decreased rather than improved. In order to determine the reason for this, the microstructure of the materials was investigated by using a light microscope (Fig. 4) and SEM (Fig. 5). Low magnification light microscope images indicated that the calcium treatment process affects some morphological properties of inclusions. While elongated inclusions were observed as well as spherical shapes in the untreated sample (Fig. 4a), the inclusions generally had a spherical shape in the calcium treated sample (Fig. 4b). TABLE 4. shows the inclusion characteristics achieved using BSE-SEM images obtained from the polished surfaces of the untreated and calcium treated steels.

According to the ImageJ software measurements (TABLE 4), the average inclusion size decreased from 3.3 µm to 1.9 µm with calcium treatment. Inclusion size has the major effect on the fatigue strength. The characteristics of the inclusions which influence toughness are volume fraction, spacing and resistance to void nucleation.

The inclusion volume fraction (f) and the number of inclusions per unit area (N_a) values were higher in calcium treated sample, while the average adjacent inclusion distance (X_0) was lower (TABLE 4). According to these results, it was observed that there were smaller, more numerous and closer inclusions in calcium treated sample than untreated sample. Micro cracks that start from hard inclusions close to each other may coalescence and turn into larger cracks.

TABLE 4

Characteristics of inclusions in untreated and calcium treated samples (f is the inclusion volume fraction, N_a is the number of inclusions per unit area on polished surfaces, X_0 is the average adjacent inclusion distance, R_0 is the true average inclusion radius)

Materials	Characteristics of inclusions				
	Average Size (µm)	f	N_a (µm^{-2})	X_0 (µm)	R_0 (µm)
Untreated	3.3 (0.7-7.0)	0.0042	0.0003	14.31	2.6
Calcium treated	1.9 (0.5-4.6)	0.0068	0.0014	6.98	1.49

SE-SEM images obtained from the polished+chemically etched surfaces of the untreated (a, b) and calcium treated samples (c, d) at low and high magnifications are presented in Fig. 5. The microstructures of the untreated and the calcium treated steel samples showed that there was no significant change in the microstructure after calcium treatment.

Fig. 6. shows detailed microstructures and EDS analysis results of the inclusions in untreated and calcium treated samples. The magnified inclusion images (Fig. 6a1, b1) supported the interpretation of the tendency of the inclusions to become spheri-

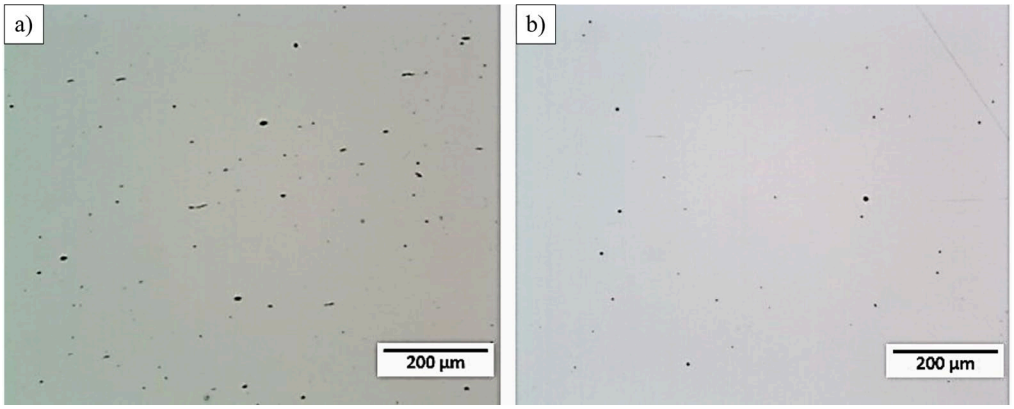

Fig. 4. Microstructures of (a) untreated and (b) calcium treated samples taken at low magnification by using a light microscope

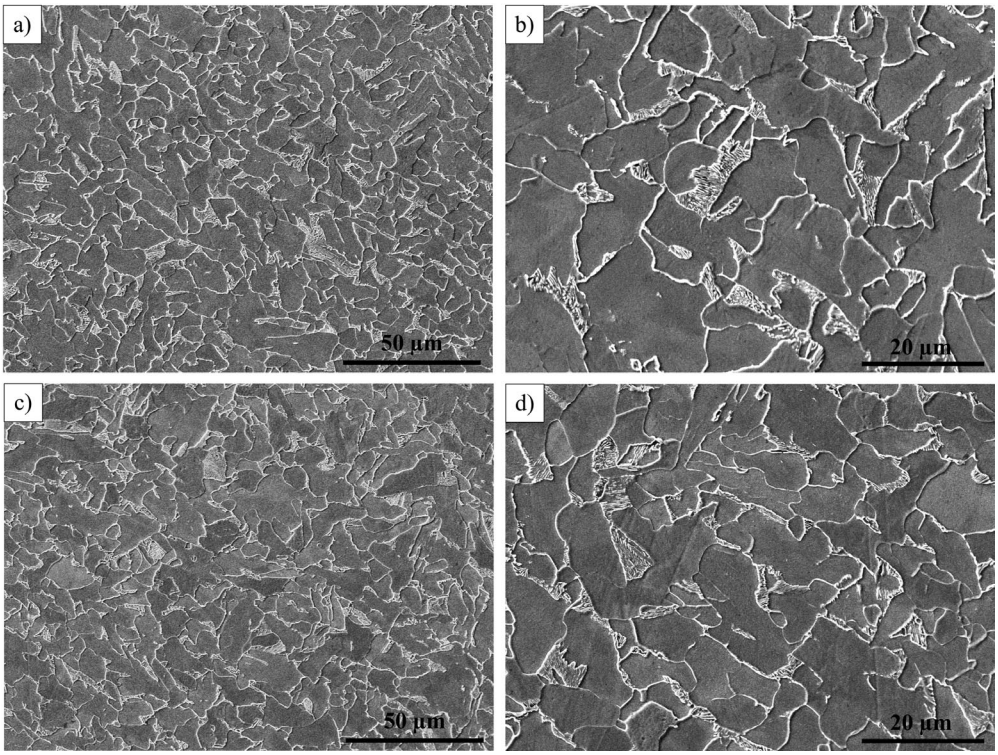

Fig. 5. SE-SEM images obtained from the polished+chemically etched surfaces of the (a, b) untreated and (c, d) calcium treated samples at (a, c) 2000× and (b, d) 4500× magnifications

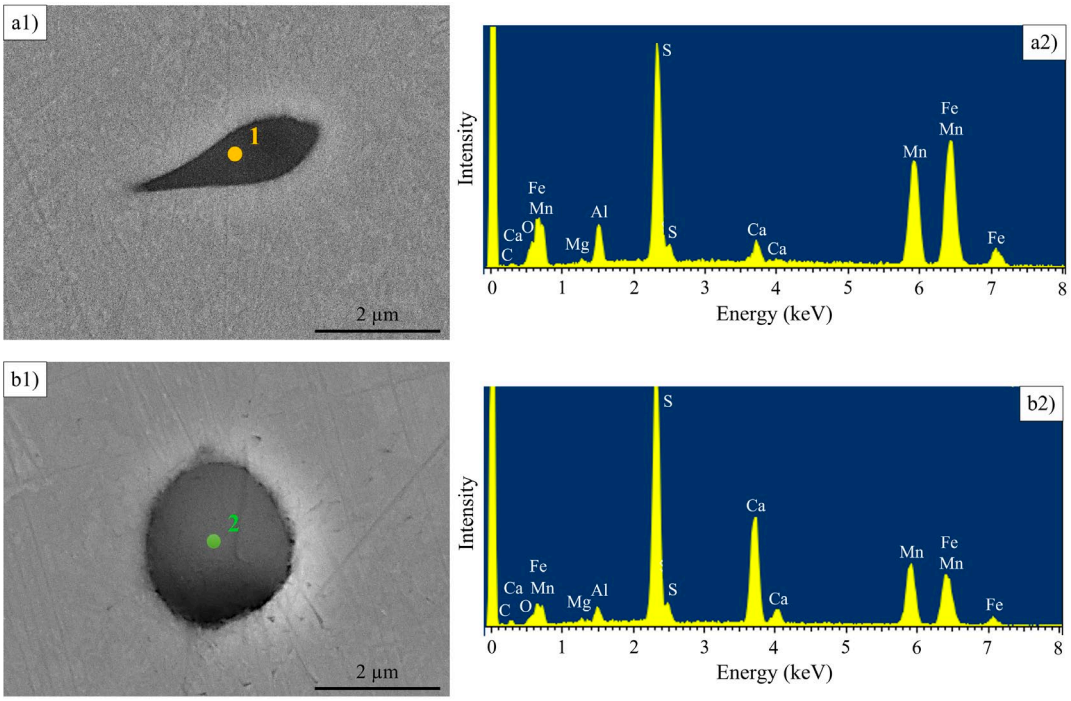

c)

Analyzed Regions	Elements (wt %)							
	Mn	Fe	S	C	Al	O	Ca	Mg
1	30.0	41.9	16.9	3.3	3.5	1.9	2.0	0.5
2	25.5	30.4	20.1	5.5	1.9	4.1	12.3	0.2

Fig. 6. (a1, b1) SE-SEM images and (a2, b2, c) EDS analyzes results including (a2, b2) spectra and (c) quantitative data of the inclusions in (a1, a2) untreated and (b1, b2) calcium treated samples

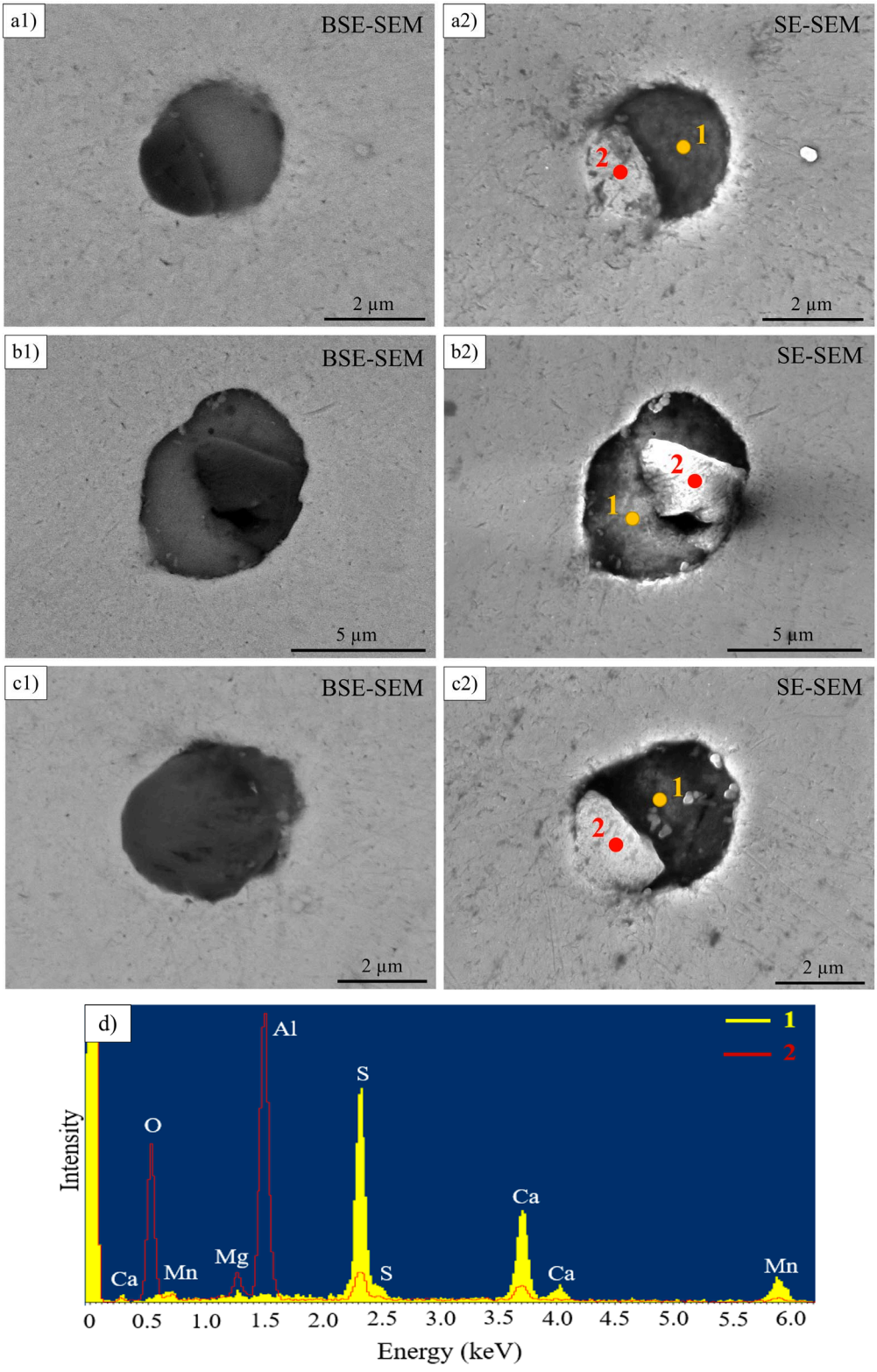

e)

Analyzed Regions	Elements (Atomic %)					
	S	Mn	Ca	O	Al	Mg
1	52.3±2.0	6.6±1.2	41.1±3.0	-	-	-
2	0.5±0.1	-	2.0±0.3	60.3±4.0	34.2±2.5	3.0±0.2

Fig. 7. (a1, b1, c1) BSE-SEM and (a2, b2, c2) SE-SEM images of the three representative inclusions in calcium treated steel. EDS analyses results including (d) EDS compared spectra and (e) quantitative data obtained from the regions marked with yellow point 1 and red point 2 in the inclusions

cal by calcium treatment based on light microscopy images. In addition, similar elements were identified in the inclusions in both samples (Fig. 6a1, b1, c).

It is observed that the amount of sulfur and oxygen has increased in the calcium treated sample (Fig. 6c). An increased sulfur content alters the inclusion balance. It becomes impossible to only bind sulfur solely in CaS. Instead, many MnS inclusions are formed though often combined with CaS, resulting in the formation of (Mn,Ca)S. (Mn,Ca)S inclusions are less ductile compared to MnS [31].

Fig. 7. shows BSE-SEM (a1, b1, c1) and SE-SEM (a2, b2, c2) images of three representative inclusions in the calcium treated sample. SE-SEM images taken from the same inclusion revealed the inclusion structure details more clearly than BSE-SEM images. In addition, EDS-SEM analyses (Fig. 7d, e) were performed on two different regions, which were observed in the structure of the three inclusions and marked with yellow number 1 and red number 2 (Fig. 7a2, b2, c2). Fig. 7d and e shows the compared EDS spectra and quantitative results, respectively. Quantitative EDS results (Fig. 7e) are the average of results from regions in the three inclusions.

Regions marked with the same number in all inclusions gave similar chemical analysis results (Fig. 7e). Alumina was observed in the most of the inclusions in the calcium treated samples. In the EDS analysis, alumina and spinel phases may coexist in grain containing Al, Mg and O (red colored number 2). All of the Mg and some Al took place in the spinel structure, while the remaining Al formed a solid phase as alumina (alumina is extremely hard). Hard inclusions are very fragile and under loads, losing their bonds with the matrix as they cannot easily change shape as the surrounding matrix, resulting in a void around them. These voids cause stress concentration, and as local stress increases the micro voids grow, coalesce, and eventually form a continuous fracture.

The SE-SEM images of the fractured surfaces taken from the fractured specimens as a result of the fatigue tests were given in Fig. 8. and Fig. 9. The untreated sample, at a maximum tensile of 400 MPa, was broken at 266.097 cycles. It is seen that the broken surface is a ductile fracture, resulting from intense plastic deformation. Cracks formed in the material due to the coalescence of micro voids can also be seen from the SEM image. There are dimples on the broken surface caused by the inclusion or separation of second phase particles. In the calcium treated sample, fracture occurred in 196.424 cycles. The untreated sample, at a maximum tensile of 350 MPa, was broken at 9.684.577 cycles. Striation marks are clearly visible on the fracture surface. In the calcium treated sample, fracture occurred in 1.048.561 cycles. When the test results and microstructures of the fracture surfaces are examined; it is seen that cracks progress rapidly in the calcium treated samples and fast fracture occurs.

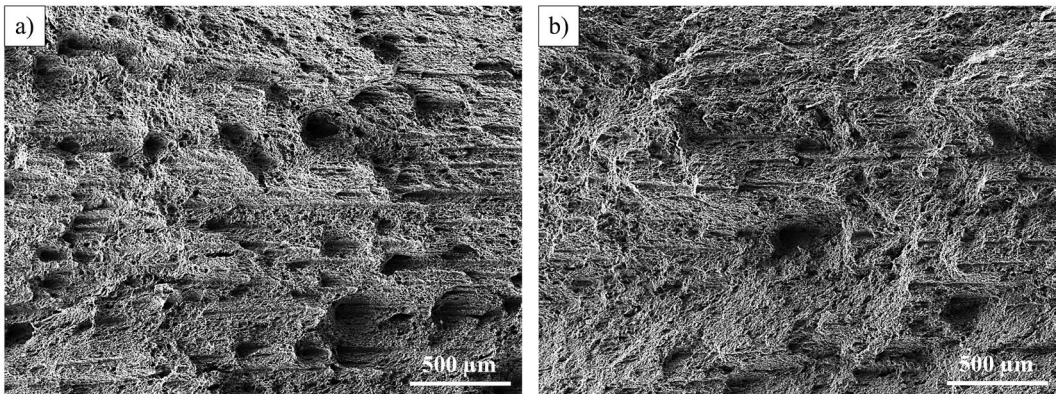

Fig. 8. SE-SEM images of fracture surfaces after the fatigue test where maximum stress of 400 MPa is applied: (a) Untreated sample. (b) Calcium treated sample

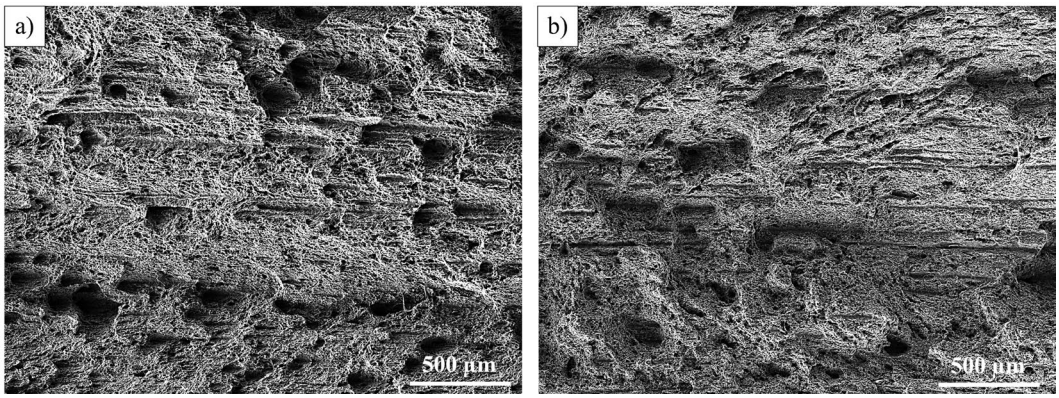

Fig. 9. SE-SEM images of fracture surfaces after the fatigue test where maximum stress of 350 MPa is applied: (a) Untreated sample. (b) Calcium treated sample

4. Conclusions

In this study, the effects of the calcium treatment process on the material's tensile strength and fatigue behavior are determined by experimental studies. For this purpose, tensile and fatigue tests have been applied to untreated and calcium treated samples. Light microscopy and SEM investigations were carried to untreated and calcium treated steels to investigate the reasons for the mechanical test results. The following results being achieved:

- When compared to untreated and calcium treated sample test results, the calcium treated samples' tensile strength increased slightly. The hard inclusions resulting from calcium treatment have caused a decrease in extension.
- The fatigue life of the calcium treated samples was lower than the untreated samples. The decrease depended on brittle inclusions that occur as a result of the calcium treatment.

Acknowledgements

This study was produced from the master's thesis number 458990, published by Anadolu University, Graduate School of Science. We would like to thank Servet Turan for his contributions to the article, to Ramazan Kale for his contributions to the experimental studies, and to Alper Çınar for his contributions to the microstructure work.

REFERENCES

[1] R. Kiessling, Metal Sci. **14** (5), 161-172 (1980). DOI: https://doi.org/10.1080/02670836.2020.12097372

[2] ASM International Handbook Committee, ASM Handbook. **1**, Properties and selection: irons, steels, and high-performance alloys, ASM International, Ohio, (1990). ISBN: 978-0-87170-377-4

[3] J. Cheng, R. Eriksson, P. Jönsson, Ironmaking & Steelmaking **30** (1), 66-72 (2003). DOI: https://doi.org/10.1179/03019230325009470

[4] A. Ghosh, CRC Press, Florida, (2001). ISBN: 9780849302640.

[5] S. Louhenkilpi, Elsevier, Pages 373-434 (2014). DOI: https://doi.org/10.1016/B978-0-08-096988-6.00007-9

[6] S.N. Singh, Metallurg. and Mat. Trans. B. **5**, 2165-2178 (1974). DOI: https://doi.org/10.1007/BF02643930

[7] L. Holappa, Ladle injection metallurgy, International Metals Reviews **27** (2), 53-76 (1982). DOI: https://doi.org/10.1179/095066082790324388

[8] D. Mu, L. Holappa, Gov. Res. Announc., Index, USA, (1993). Report No: PB93-179471/XAB

[9] A.W. Cramb. In: C.L. Briant, editor, CRC Press, Florida, (1999). ISBN: 9780203751190

[10] L. Zhang, B.G. Thomas, The Iron and Steel Inst. of Japan Int. **43**, 271-291 (2003). DOI: https://doi.org/10.2355/isijinternational.43.271

[11] R.J. Fruehan, Iron and Steel Soc., Pennsylvania, (1985). ISBN: 0932897010

[12] R.J. Fruehan, 11th ed., AISE Steel Foundation, Pittsburgh, (1998). ISBN: 978-0-930767-02-0

[13] E.T. Turkdogan, The Institute of Materials, London, (1996). ISBN: 1861250045, 9781861250049

[14] Y. Kaçar, Thesis, Istanbul Technical University, (2011). ISBN: http://hdl.handle.net/11527/9721

[15] X. Li, X. Long, L. Wang, S. Tong, X. Wang, Y. Zhang, Y. Li, Materials (Basel) **13** (3), 619-631 (2020). DOI: https://doi.org/10.3390/ma13030619

[16] P. Juvonen, Thesis, Helsinki University of Technology, (2004). ISBN: 951-22-7423-X

[17] Z. Deng, M. Zhu, Steel Res. Int. **84** (6), 519-525 (2013). DOI: https://doi.org/10.1002/srin.201200250

[18] S. Abraham, R. Bodnar, J. Raines, Y. Wang, J. of Iron and Steel Res. Int. **25** (2), 133-145 (2018). DOI: https://doi.org/10.1007/s42243-018-0017-3

[19] J. Ma, B. Zhang, D. Xu, E.H. Han, W. Ke, Int. J. of Fatigue **32** (7), 1116-1125 (2010). DOI: https://doi.org/10.1016/j.ijfatigue.2009.12.005

[20] S.X. Li, Int. Mat. Rev. **57** (2), 92-114 (2012). DOI: https://doi.org/10.1179/1743280411Y.0000000008

[21] T. Lipiński, A. Wach, Arch. of Metall. and Mat. **60** (1), 65-69 (2015). DOI: https://doi.org/10.1515/amm-2015-0010

[22] J. Fagerlund, L. Kamjou, American Gear Manufacturers Association, Virginia, NO: 17FTM15 (2017).

[23] C. Gu, M. Wang, Y. Bao, F. Wang, J. Lian, Metals **9** (4), 476 (2019). DOI: https://doi.org/10.3390/met9040476

[24] A.L.V. da Costa e Silva, J. of Mat. Res. and Tech. **8** (2), 2408-2422 (2019). DOI: https://doi.org/10.1016/j.jmrt.2019.01.009

[25] M. Wang, W. Xiao, P. Gan, C. Gu, Y.P. Bao, Metals **10** (2), 201, 1-15 (2020). DOI: https://doi.org/10.3390/met10020201

[26] W.M. Garrison, A.L. Wojcieszynski, Materials Science & Engineering A **464**, 321-329 (2007). DOI: https://doi.org/10.1016/j.msea.2007.02.015

[27] M.F. Ashby, R. Ebeling, Trans. TMS-AIME **236**, 1396-1404 (1966).

[28] E.E. Underwood, Addison-Wesley Publishing Company, California+London, p. 85 (1970). ISBN: 0201076500

[29] E.E. Underwood, Addison-Wesley Publishing Company, California+London, p. 111 (1970). ISBN: 0201076500

[30] J.E. Hilliard, L.R. Lawson, Springer-Science+Business Media, B.V., Netherlands, (2003). ISBN: 978-90-481-6455-4

[31] N. Ånmark, A. Karasev, P.G. Jönsson, Materials (Basel) **8** (2), 751-783 (2015). DOI: https://doi.org/10.3390/ma8020751